Journal of Molecular Liquids 392 (2023) 123425

Contents lists available at ScienceDirect

Journal of Molecular Liquids

journal homepage: www.elsevier.com/locate/molliq

Enhanced connectivity and mobility in liquid water: Implications for the high density liquid structure and its onset

Chiara Faccio [a], Nico Di Fonte [b], Isabella Daidone [b,*], Laura Zanetti-Polzi [c,*]

[a] Scuola Normale Superiore, Piazza dei Cavalieri 7, Pisa, 56126, Italy
[b] Department of Physical and Chemical Sciences, University of L'Aquila, via Vetoio (Coppito 1), L'Aquila, 67010, Italy
[c] Center S3, CNR-Institute of Nanoscience, Via Campi 213/A, Modena, 41125, Italy

ARTICLE INFO

Keywords:
LDL/HDL water
Widom line
Water network
Node total communicability
Graph theory

ABSTRACT

In this work, we investigate simulated liquid water at ambient pressure in both stable and metastable supercooled conditions by means of a new order parameter we recently proposed, namely the node total communicability (NTC), based on graph theory concepts. We show that this order parameter is able to identify the two liquid states differing in density, the LDL- and HDL-like states, in simulation conditions at which both states coexist. We also show that NTC is able to capture both the structural and dynamic differences between the two states, being correlated with both the local density and the mobility of water molecules within the network. In addition, we further investigate the high connectivity patches we previously identified as characteristic of the HDL-like state. We show that these extended patches are composed of molecules with an increased local density and mobility, packed in a highly connected network. The formation of these highly connected networks is characterized by a fast dynamics, with mobile molecules entering and exiting the patches. Interestingly, we observe small highly connected patches also at low temperatures, where the prevailing state is LDL-like. We show that the small-to-large patches transition is related to the Widom line crossing and we suggest that the small highly connected patches at low temperatures might function as initial sites for the formation of extended HDL-like regions characteristic of the highest temperatures.

1. Introduction

The properties of water are the subject of extensive investigation in many research fields such as physics, biology, and chemistry. Nonetheless, the microscopic structure of liquid water, even at ambient conditions, is still under hot debate. As a matter of fact, different local molecular arrangements appear in water at ambient pressure and temperature, accompanied by spatio-temporal fluctuations in the hydrogen bond (HB) network [1]. The scenario is even more complicated at the pressure and temperature conditions where water can exist as a metastable supercooled liquid below its equilibrium melting temperature. The well known anomalies in water thermodynamics and dynamics are in fact amplified upon supercooling, and vast research was performed to gain insights into the origin of these anomalies [2]. Among other possible thermodynamic scenarios [2,3] (i.e., the stability-limit conjecture [4], the critical-point-free scenario [5,6] and the singularity-free scenario [7,8]), the liquid–liquid critical point (LLCP) hypothesis [9] is the leading conjecture to explain water anomalies. According to this thermodynamic scenario, the marked increase in the thermodynamic response functions upon supercooling is due to the existence of a LLCP in the conventionally called "no man's land", i.e., the phase-diagram region below the temperature of homogeneous nucleation temperature and above the crystallization line [10]. This implies the existence of a first order liquid-liquid phase transition (LLPT) between two phases: the low- (LDL) and high-density liquid (HDL). Beyond the LLCP, the locus of extrema of the correlation length defines the Widom line [3]. In this region of the phase diagram, the LDL and HDL coexist in a fluctuating equilibrium. Despite several experimental works supporting the LLCP scenario [1,11–14], a conclusive experiment proving the existence of a second critical point in water could not be performed yet, due to fast crystallization in the region where the LLCP should be located. On the other hand, a large body of theoretical and computational works have been performed exploring the "no man's land" [15–18] (see also Gallo et al. [2] and references therein). The structural, thermody-

* Corresponding authors.
E-mail addresses: isabella.daidone@univaq.it (I. Daidone), laura.zanettipolzi@nano.cnr.it (L. Zanetti-Polzi).

https://doi.org/10.1016/j.molliq.2023.123425
Received 4 August 2023; Received in revised form 24 September 2023; Accepted 23 October 2023
Available online 29 October 2023

namic and dynamic properties of supercooled and ambient conditions water have been widely investigated by means of molecular dynamics (MD) simulations of several water models, as well as by means of analytic thermodynamic models. Most of the latter rely on a two-state description of liquid water, hypothesizing an equilibrium between LDL-like and HDL-like local environments at the molecular level [19–26]

Besides differing in density, the LDL-like and HDL-like states also feature different local structures: the LDL-like structure resembles that of ice, with four nearest neighbors in a regular tetrahedral arrangement; the HDL-like structure is characterized by a distorted HB pattern with a fifth nearest neighbor (the so-called interstitial water molecule). Despite these structural differences, the unambiguous assignment of a specific molecule to either a state or the other is not trivial, and a number of structural order parameters have been developed aiming at characterizing simulated water at different pressure and temperature conditions. These structural descriptors, such as the local structure index (LSI) [27], d_5 [28], ζ [29], V_4 [30], Ψ [31] and the node total communicability (NTC) we recently proposed [32], are used to infer the structural features of liquid water in a two-state picture. It was shown, for example, that the HB network of LDL-like molecules is characterized by an equal number of pentagonal and hexagonal rings [33], that in the HDL-like state interstitial water molecules arise from the folding back of long HB rings [34], and that the HDL-like state is not homogeneous but rather features patches of water molecules characterized by a particularly high connectivity [32].

Besides the well known thermodynamic anomalies, water also shows dynamic anomalies, such as the counter-intuitive fact that the denser HDL-like molecules have a larger mobility. Upon cooling, water dynamics shows a crossover from a fragile-liquid behavior at high temperature to a strong-liquid behavior at low temperatures [3]. This behavior has been also interpreted in the framework of the two-state model of water as a strong-to-strong transition, i.e., as the switch between two distinct Arrhenius regimes in the two distinct liquid states [23,35,36]. Water dynamics is also characterized by the so-called “dynamical heterogeneities”, i.e., the existence of regions with different mobility, with localized patches of molecules showing an increased mobility [37]. Regions with different mobility have been connected to regions with different structural features. For example, a higher number of nearest neighbors is associated to an increased mobility [38], less mobile regions are characterized by an increased tetrahedrality [35] and the “defect propensity”, quantifying the tendency of a molecule to assume distorted configurations, correlates with its dynamic propensity [39]. Therefore, the dynamics of water strongly depends on the local density and structure. This, together with the observation that the fragile-to-strong crossover occurs at the Widom line [2], suggests that there is a strong connection between the dynamic and thermodynamic anomalies in supercooled water. Interestingly, a relevant role of the dynamic properties in driving ice nucleation has been recently proposed [40]. Nonetheless, the interplay between structural, thermodynamic and dynamic properties in affecting the behavior of supercooled water is still under debate.

Aiming at clarifying the link between structure and dynamics, the relationship between local structural ordering and dynamical heterogeneities was investigated in model glass forming systems [41–46]. Efforts have been also devoted to find order parameters with a strong correlation with dynamics. With an unsupervised machine learning approach, that does not use any dynamical information, a structural order parameter was obtained strongly correlating with dynamical heterogeneties in three glass forming systems [47]. In addition, Tanaka and coworkers found a correlation between the molecular mobility in simulated water and the coarse-grained version of the order parameter ζ, ζ_{CG} [23,36]. The fact that a correlation with the dynamics is observed only when the ζ parameter is averaged on the first hydration shell, was explained by observing that the dynamics of a water molecule is non local, and intrinsically coupled to that of its neighbors [36]. The importance of going beyond a purely local description to properly describe the dynamics of supercooled liquids was further stressed later on [48].

In our recent paper [32], we proposed an order parameter inspired by concepts from graph theory, namely the node total communicability, to investigate the structure of liquid water. The peculiarity of this order parameter is that it takes into account not only the first hydration shell of the target molecule, but also medium- to long-range effects. By computing this order parameter on MD simulations of the TIP4P/2005 water model [49] along the 1950 bar isobar that crosses the liquid–liquid coexistence line, we showed that the NTC is able to properly identify the LDL-like and HDL-like water phases. In addition, the NTC showed in the HDL-like phase the existence of patches of water molecules characterized by a high connectivity and an increased number of interstitial water molecules.

In this work, we extend the investigation of liquid water with the NTC by analyzing several temperatures along the 1 bar isobar, that crosses the Widom line. We test the ability of the NTC in identifying the LDL- and HDL-like structures in simulation conditions at which both states coexist. In addition, we also investigate the correlation between the NTC and the dynamical properties of the system. We also further investigate the high-connectivity patches we previously identified, and their temperature dependence, in terms of i) number of molecules in the patches, ii) mean lifetime of the patches and iii) mobility of the molecules inside and outside the patches.

2. Methods

2.1. Graph theory and centrality measures

In this section, we recall some basic notions from graph theory. A more exhaustive description can be found in our previous works [32,50] or in the work of Estrada [51], but we briefly report it for setting the notation and self-containing the paper.

A graph G consists of a pair of finite sets (V, E), where V is the set of nodes $V = \{v_1, \cdots, v_N\}$ and $E \subseteq V \times V$ is the set of the edges. The symbol $e_{ij} = (v_i, v_j) \in E$ indicates that in the graph there is an edge from the node v_i to the node v_j. If all the edges in a network are without orientation, i.e. $e_{ij} = (v_i, v_j) = (v_j, v_i) = e_{ji}\ \forall e_{ij} \in E$, the graph is called *undirected*, otherwise it is a *directed* graph. In a graph, each edge e_{ij} can be endowed with a positive number $w_{i,j}$, called the weight. This quantity can represent, for instance, the physical distance between the two nodes, or the strength of their link. In this case, the graph is called *weighted*. Otherwise, if only the existence of a connection between nodes is taken into account, the weight of each edge is set to 1, and the graph is called *unweighted*.

The *adjacency matrix* associated with a graph G is a squared matrix A of dimension $N \times N$, where N is the number of nodes in the graph. The entry a_{ij} is nonzero if and only if there exists an edge from the node v_i to the node v_j, and in this case $a_{ij} = w_{ij}$. Clearly, if the graph is undirected, the associated adjacency matrix is symmetric, and if G is unweighted, A is binary. In this paper, we consider only undirected, unweighted graphs and without self-loops, i.e. edges of the form $e_{ii} = (v_i, v_i)$.

A *walk* between two nodes v_i and v_j is a sequence of edges in G (not necessarily distinct) of the form $e_{ip}, e_{pq}, \ldots, e_{sr}, e_{rj}$. If $i = j$ the walk is closed. Given a positive integer k, the entry $[A^k]_{ij}$ (the entry in position {i j} of the k-th power of A) is equal to the number of walks of length k between the nodes v_i and v_j. A *path* is a walk in which each node is visited exactly once. A graph is *connected* if given a node, any other node in the graph can be reached by following a path in G. The *degree* of a node v_i (indicated by $deg(v_i)$) is the number of edges that are connected to that node, or equivalently it is the number of vertices that are joined to v_i by an edge.

In our previous works [32,50], we presented a new order parameter based on a centrality measure, the node total communicability (NTC), to differentiate the two forms of liquid water at high pressure. A *centrality measure* is a quantity used to identify the “most important” nodes in a

graph. The meaning of "important node" depends on the properties of the graph that we consider. In this work we examine the *degree centrality* and the NTC. The degree centrality is the simplest one, and it is defined as the degree of the nodes, so it only looks at the adjacent nodes to each vertex. It is computed by multiplying the matrix A for the vector of all ones $\mathbf{1}$, i.e. $deg(v_i) = [A\mathbf{1}]_i$. On the other hand, the NTC [52,53] does not only consider the first neighbors of a node, but it also takes into account medium-long range effects. Let $\beta > 0$, the NTC of the node v_i is defined as

$$NTC(v_i) = [e^{\beta A}\mathbf{1}]_i = \sum_{k=0}^{\infty} \frac{\beta^k}{k!}[A^k\mathbf{1}]_i = 1 + \beta deg(v_i) + \frac{\beta^2}{2!}[A^2\mathbf{1}]_i + \frac{\beta^3}{3!}[A^3\mathbf{1}]_i + \cdots \quad (1)$$

where $\mathbf{1}$ is again the vector of all ones. Therefore, the NTC of a node v_i considers all the walks between v_i and the other nodes in the graph, with the contribution of each walk of length k (with $k = 1, 2, \dots$) weighted by the factor $\frac{\beta^k}{k!}$. In this way, the longer walks are penalized through less weight, and the parameter β can be used to give more or less weight to these longer walks. For small values of β the obtained ranking of the nodes is equal to the degree centrality ranking, while for $\beta \to \infty$ this measure is equivalent to the eigenvector centrality [54]. If the graph is connected, the *eigenvector centrality* [55] of a node v_i is defined as the i-th entry of the eigenvector $\mathbf{p}$ associates with the largest eigenvalue of A, denoted by $\rho(A)$ (by the Perron-Frobenius Theorem, $\rho(A)$ is a positive and simple eigenvalue of A and its eigenvector $\mathbf{p}$ is unique (up to normalization) and positive). In this paper, we do not consider this centrality measure because we found that it is not well-suited to differentiate the two phases in liquid water, see [32] for details.

For the computation of the NTC, we use $\beta = 1$. As was shown in [32,50], this is a default value for the node total communicability, which however has proved to be useful in recognizing the two liquid forms of water in the supercooled region at high pressure. As previously shown [32], with this value of β we give a non negligible weight to each walk of length $k \leq 4$ (each walk of length k is weighted by the factor $\frac{\beta^k}{k!}$). In this way, we give more weight to the walks that include molecules within ≈ 1 nm from the target molecule, i.e. within the fourth hydration shell as obtained from the $g_{OO}(r)$, the O···O-pair distribution function. Nonetheless, the NTC uses all the walks of length k, with $k = 1, ..., \infty$. Therefore, the cumulative contribution to the NTC of the walks of length $k \geq 5$ is non negligible. This allows us to include medium-long range effects in the computation of the NTC, beyond the fourth hydration shell. Indeed, the distance out to which there is (temperature-dependent) structure in the $g_{OO}(r)$ was shown to extend up to ≈1.5-1.7 nm [56]. Moreover, both experimental [1] and simulated [57] data suggested a spatial extent on the order of 1 nm diameter for density heterogeneities in ambient water, i.e. the distance up to which walks have a more relevant weight in the NTC calculation.

2.2. Molecular dynamics simulations

We perform molecular dynamics (MD) simulations of water at 1 bar at 12 different temperatures (see Fig. 1 and Table 1 in the Supporting Information, SI, for details on the simulation lengths) using the TIP4P/2005 water model [49] that is widely used in the simulation of both pure water and aqueous solutions and exhibits a metastable liquid–liquid critical point in deeply supercooled conditions. Depending on the details of the simulation conditions, the second critical point for TIP4P/2005 has been located at 1600-1750 bar and 177-182 K [21,22,58–60], with a very recent estimate at 1860 bar and 172 K [18]. The simulation conditions we use here are consistent with those of Biddle et al. [22], who estimated the second critical point at 1700 bar and 182 K. All MD simulations were performed in the NPT ensemble with the 5.1.2 version of the GROMACS software [61] using a cubic simulation box containing 710 water molecules. Temperature and pressure were kept constant by using the velocity rescaling temperature coupling

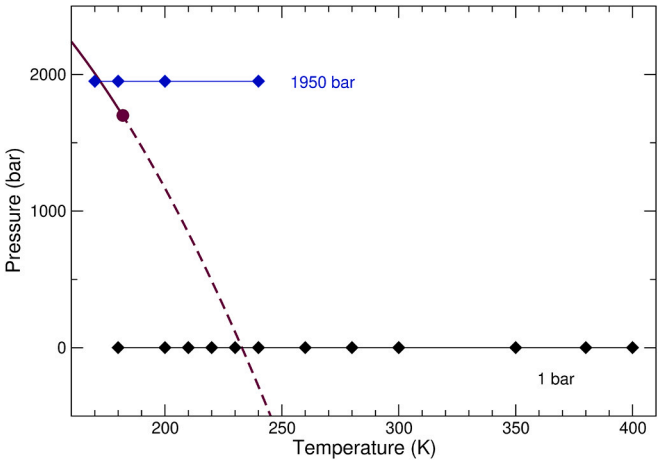

Fig. 1. Black filled diamonds: MD simulation temperatures along the 1 bar isobar. Blue filled diamonds: previously investigated temperatures along the 1950 bar isobar [32]. Dark red: liquid-liquid coexistence line (solid), Widom line (dashed) and LLCP (filled circle) as estimated by the two-structure equation of state (TSEOS) for the TIP4P/2005 water model by Anisimov and coworkers [21].

[62] and the Parrinello–Rahman barostat with 2 ps relaxation times [63]. Periodic boundary conditions were used, long range electrostatic interactions were treated with the particle mesh Ewald method [64] with a real space cutoff of 0.9 nm and for short range interactions a cutoff radius of 0.9 nm was employed. All bonds were constrained using the LINCS algorithm [65] along with a 2 fs time step.

2.3. Construction of the graphs

Given a MD trajectory, to apply the tools of graph theory, we need to transform the information contained in the simulations into graphs. For this purpose, for each frame of the trajectory, we extract the coordinates of the atoms. In this work, we implement the same strategy proposed in [32,50], in order to compare the results under different pressures. The oxygen atoms compose the nodes of our graph, while the edges represent the interactions between the molecules. In particular, we consider two nodes (i.e., oxygen atoms) as connected if their distance is less than or equal to 0.35 nm, see [32] for details on choosing this threshold. In this way, we get undirected and unweighted graphs.

Since in the MD simulations periodic boundary conditions are used, we employ in constructing the graph the minimum image convention to compute the distance between two oxygen atoms.

The companion software, which is used to construct the networks from trajectories and to analyze them using graph theory concepts, is available in the GitHub repository (https://github.com/ChiaraFaccio/WaterNetworks). The code uses the following packages/libraries: NetworkX 2.6.3 module [66] in Python 3.7, the MDAnalysis library [67,68], the Python package NetworkSNS [69] and the open-source packages NumPy [70], SciPy [71], and Matplotlib [72].

3. Results and discussion

In our recent work [32], we presented the use of the node total communicability (NTC) as a new order parameter to identify the two liquid phases of water differing in density. Our previous work focused on the high pressure region of the phase diagram where the liquid-liquid coexistence line is crossed; in the present work we use the same order parameter to investigate the properties of liquid water at several temperatures at ambient pressure, where the Widom line is crossed (Fig. 1). We use MD simulations at 12 different temperatures of the TIP4P/2005 water model [49] along the 1 bar isobar that was previously shown to cross the Widom line between 230 and 235 K [21,26].

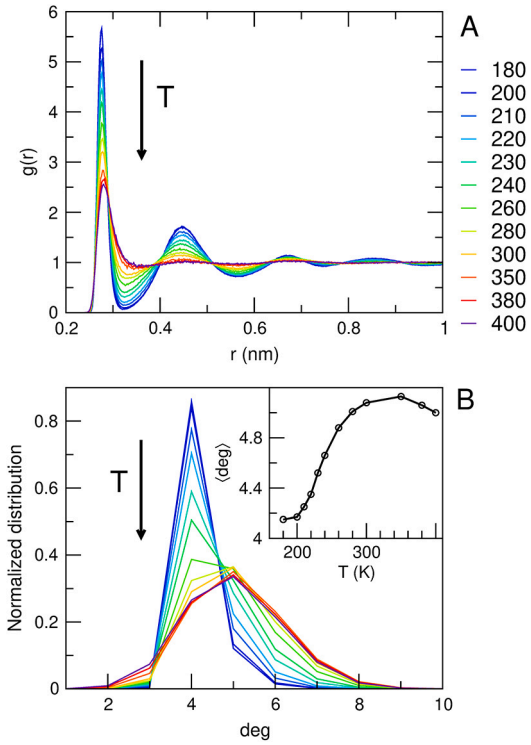

Fig. 2. A: Pair radial distribution functions (g(r)) for the O···O contacts. B: Normalized distribution of the degree centrality (deg). Inset in B reports the average degree centrality as a function of the temperature.

As anticipated from the behavior of the pair radial distribution functions, g(r), for the O···O contacts along the 1 bar isobar (Fig. 2A), the number of first-shell neighbors, as obtained from the degree centrality (Fig. 2B), increases with the temperature with an inflection point around the Widom line temperature and a slight decrease at the two highest temperatures approaching the liquid-gas phase transition (the boiling temperature for TIP4P/2005 is 401 K [73]). As already observed at 1950 bar [32], the NTC distributions (Fig. 3A) show a more marked variation upon raising the temperature with respect to the degree centrality while maintaining the same temperature trend (inset of Fig. 3A). At the lowest temperatures the distributions are very sharp and peaked at low NTC values; by increasing the temperature the distributions are considerably broader and their mode is progressively shifted to higher NTC values (Fig. 3B).

As pointed out in our previous work [50], the graphs in the LDL phase in the supercooled region are close to being four-regular graphs. In an undirected d-regular graph, every node has the same value of degree centrality $deg(v_i) = d$, and, therefore, the same value of NTC, $NTC(v_i) = e^{\beta d}$. In fact, as shown in Fig. 3A, the modes of the distributions at the lowest temperatures are approximately around $e^4 \approx 54.60$. The similarity between the LDL-like state connectivity and that of a four regular graph shows that the LDL-like state is very homogeneous in terms of connectivity, with an almost 4-regular structure resembling the tetrahedral arrangement of the parent crystal [74].

Interestingly, the distribution at the lowest temperature (180 K), at which TIP4P/2005 is expected in a single LDL-like state, well matches the distribution obtained at 1950 bar for the pure LDL-like state at 170 K. In addition, the distribution at 300 K (with TIP4P/2005 almost fully HDL-like) intersects the distribution at 180 K (with TIP4P/2005 almost fully LDL-like) at NTC = 95 (Fig. 3C), i.e. the same NTC value at which, at 1950 bar, there is the intersection between the distribution at 170 K (pure LDL-like state) and 180 K (pure HDL-like state). Therefore, as previously done at 1950 bar [32], we choose the value NTC = 95 to distinguish between LDL- and HDL-like molecules also at 1 bar: for NTC≤95 a water molecule is assigned to the LDL-like state and for NTC>95 to the HDL-like state. As a further test of the reliability of this choice, we report in Fig. 4A the probability of having NTC = 95 as a function of the temperature. It can be observed that there is a maximum between 230 and 240 K, i.e., at the expected Widom line temperature [21,26]. As the Widom line temperature has been defined in that previous work as the temperature at which there is equal fraction of LDL- and HDL-like molecules, the maximum in the above trend shows that the choice NTC = 95 as a threshold properly identifies the temperature at which the overlap between the LDL- and HDL-like populations is maximum. This result also suggests that the chosen NTC threshold is roughly pressure-independent, allowing the usage of the NTC as an order parameter along different isobars without any adjustment.

We use therefore the NTC = 95 threshold to compute the LDL fraction along the 1 bar isobar (Fig. 4B). It can be observed that, differently from the 1950 bar isobar along which, consistently with the coexistence line crossing, a sudden jump occurs in a small (10 K) temperature interval, along the 1 bar isobar the LDL fraction continuously decreases by increasing the temperature, consistently with the Widom line crossing. It can also be observed that the 0.5 LDL fraction is at 230 K, i.e., in agreement with what previously predicted for TIP4P/2005. At the lowest temperature (180 K) water is almost fully LDL-like (LDL fraction = 0.95) while it is almost fully HDL-like from 280 K (LDL fraction between 0.05 and 0.10). In Fig. 4B we compare the LDL fraction obtained using the NTC as order parameter with that obtained using two different order parameters: ζ and ψ. Given a molecule i, to compute the quantity ζ_i, its closest not hydrogen-bonded neighbor j' and its last hydrogen bonded neighbor j'' are identified. Then, $\zeta_i = r_{j'i} - r_{j''i}$, where, in general, r_{ji} represents the distance between the molecules j and i [29]. ψ is a recently introduced order parameter based on the observation that the distance between pairs of molecules separated by 4 links along the HB network (chemical distance D = 4) is different in the LDL- and HDL-like states. The quantity ψ_i of a molecule i is defined as the minimal distance between molecules at chemical distance D = 4 from i [31]. To define the LDL-like fraction using these two order parameters, we use as threshold to separate the two states the crossing point between the distributions obtained at the lowest and highest temperature. It can be observed that while the three order parameters provide similar estimates of the temperature at which the LDL fraction is 0.5 (see caption of Fig. 4), both ζ and ψ provide a slightly lower LDL fraction at low temperatures and a rather higher LDL fraction at high temperatures. This is particularly evident in the temperature interval between 260 and 350 K. The origin of this difference likely arises from the different "locality degree" of the three order parameters. As a matter of fact, despite both ζ and ψ take into account second-shell effects, they essentially depend on the distance between the target molecule and its very first neighbors. On the contrary, the NTC takes into account medium- to long-range effects, accounting for the connectivity of the whole hydration shell of the target molecule [32]. At high temperatures there will be molecules with a local tetrahedral LDL-like arrangement that are surrounded by HDL-like molecules. These molecules will be identified as LDL-like by ζ and ψ, but will be identified as HDL-like by the NTC because their overall connectivity (accounting for both their connectivity and that of their neighbors) will be that of HDL-like molecules. We also note that the inclusion of nearest neighbors effects by using the coarse grained version of ζ was also shown to provide a steeper variation of the LDL fraction as a function of the temperature [23,36]. In addition, the temperature trend of the LDL fraction provided by the NTC is quite in good agreement with that provided by our recently proposed thermodynamic model [26,75]. According to that model, the minimum number of water molecules necessary to define a cluster that can be found in either the LDL-like or the HDL-like thermodynamic state is around 10 at 1 bar, suggesting that the local tetrahedral LDL-like arrangement of a single molecule is not sufficient to confer to that molecule an LDL-like character.

The importance of taking into account the properties of the neighbors of a molecule to properly define its own properties has been indeed

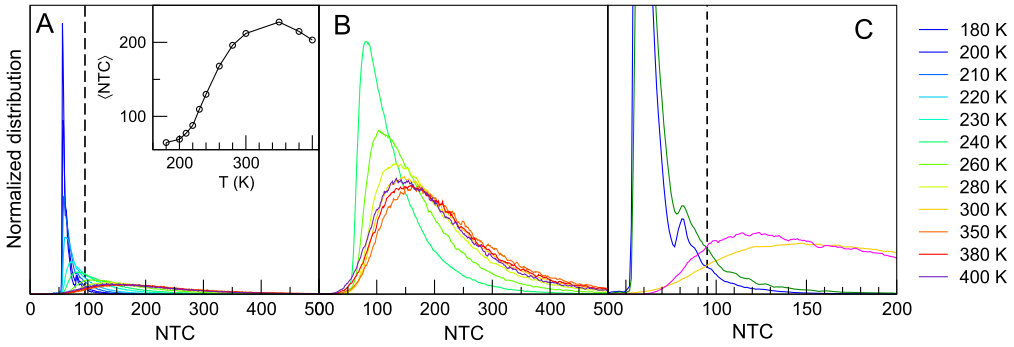

Fig. 3. Normalized distribution of the node total communicability (NTC). A: all temperatures, B: temperatures above the Widom line temperature (i.e., from 240 K to 400 K), C: comparison between the LDL- and HDL-like distributions at 1 bar (blue, 180 K, and orange, 300 K) and at 1950 bar (green, 170 K, and magenta, 180 K). The black dashed lines in A and C mark the NTC = 95 threshold. Inset in A reports the average NTC as a function of the temperature.

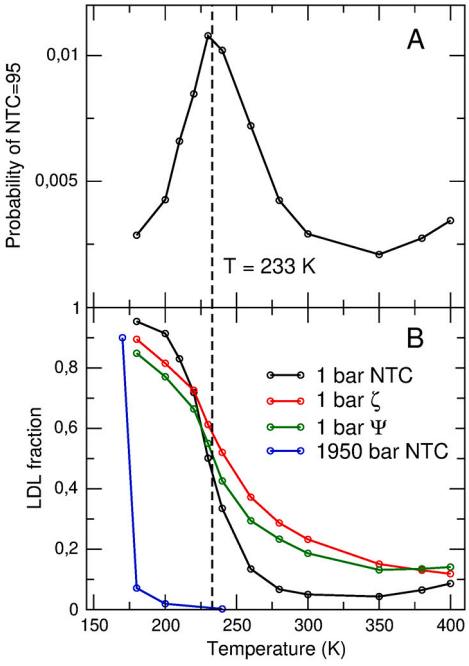

Fig. 4. A: Probability of NTC = 95 as a function of the temperature. B: LDL fraction as a function of the temperature as obtained by defining the LDL-like state according to the NTC at 1 bar (black) and 1950 bar (blue), the ζ order parameter (red) and the ψ order parameter (green). At 230 K the LDL fraction at 1 bar provided by the three order parameters is 0.50, 0.61 and 0.55 for NTC, ζ and ψ, respectively. The black dashed line marks the Widom line temperature as obtained by the TSEOS model of Anisimov and coworkers [21].

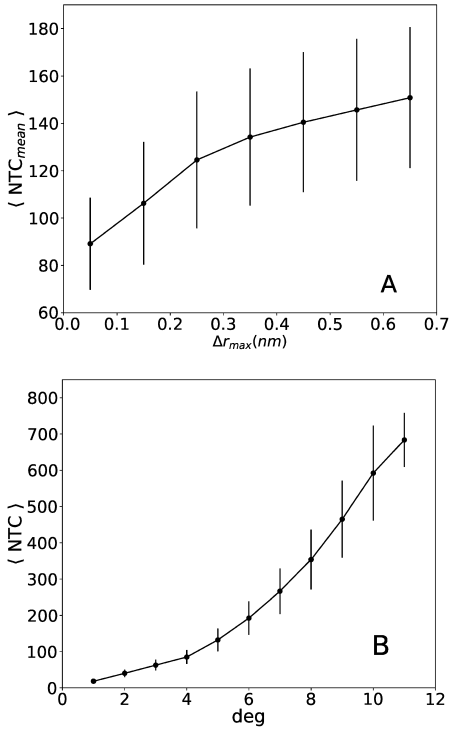

Fig. 5. A: Average value of $NTC_{mean}(\tau)$ as a function of different intervals of the mobility $\Delta r_{max}(\tau_4)$ at 230 K. B: Average value of NTC as a function of different values of the degree centrality at 230 K. In A and B, the error bars are obtained considering the standard deviation.

already pointed out. In particular, it was shown that the dynamics of a water molecule cannot be determined locally because it is strongly coupled to that of its neighbors [23,36]. With the same procedure used by Shi et al. [36], we show that the NTC also reports on the dynamical properties of water: a higher connectivity corresponds to a higher mobility. Along the MD simulation at 230 K (i.e., just below the Widom line temperature), we calculate the mobility of each water molecule i as $\Delta r_{max,i}(\tau_4)$, i.e., the maximum distance the molecule i travels in the time interval τ_4. We choose $\tau_4 = 30$ ps because the translational four-point susceptibility $\chi_4^T(t)$ maximizes at $t = \tau_4 = 30$ ps (see section 2 in the SI). In the same time interval we also compute the average NTC value, $NTC_{mean,i}(\tau_4)$, for the molecule i. In Fig. 5A, we report $\langle NTC_{mean} \rangle$, i.e. the average of $NTC_{i,mean}(\tau_4)$ on the water molecules belonging to different mobility intervals $\Delta r^k_{max}(\tau_4) \in (k, k+1)$ Å for $k = 0, \ldots, 6$. It can be observed that the two quantities are correlated, showing that a higher NTC corresponds to a higher mobility. It has to be underlined that, by definition, the NTC also reports on the local connectivity of the node (being the degree the first term in its expansion, see Eq. (1)). As a matter of fact, as shown in Fig. 5B, the molecules with a higher degree centrality (or local density) also show on average higher NTC values. Therefore, the NTC value of a molecule depends on the combination of both its local structural properties and its medium-range dynamical properties. It was previously stated that the failure of two-state approaches in describing water dynamics has to be attributed to the poor capability of order parameters to describe the dynamical anomalies of water [23]. In the same work, Tanaka and coworkers show that while the standard "local" ζ order parameter well correlates with the local density, only its "non-local" coarse-grained version ζ_{CG} correlates with the mobility. We therefore analyze the correlation at the single molecule level of the NTC with both the local density (using the degree centrality) and the mobility (using $\Delta r_{max,i}(\tau_4)$) The correlation at the single molecule level between the NTC and the local density is comparable with that between ζ and the local density (correlation coefficient $\approx$0.8 in both cases). Interestingly, the correlation at the single molecule

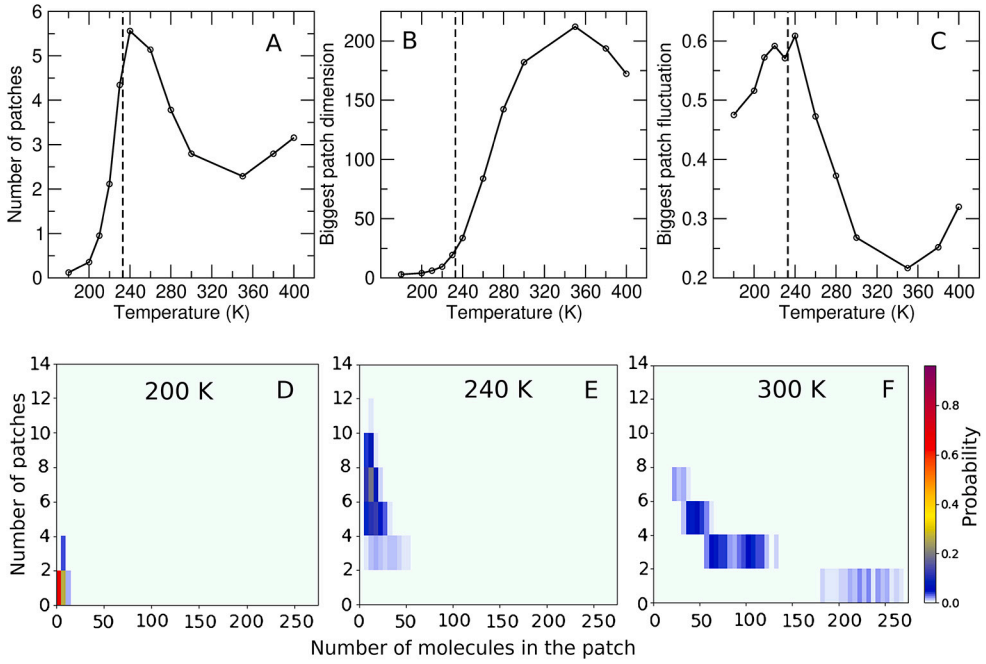

Fig. 6. A: Average number of patches containing m≥5 molecules as a function of the temperature. B: Average number of molecules in the biggest patch as a function of the temperature. C: Fluctuation of the dimension of the biggest patch as a function of the temperature. The fluctuation is obtained as the ratio $\sigma_{BP}/\langle BP\rangle$, with BP indicating the biggest patch dimension and average and σ calculated along the MD trajectory at each temperature. D-F: Two-dimensional plots reporting the number of patches as a function of the number of molecules in the patch for three different temperatures: below the Widom line temperature (200 K, panel D); around the Widom line temperature (240 K, panel E) and above the Widom line temperature (300 K, panel F).

level between the NTC and the mobility is comparable to that between ζ_{CG} and the mobility (correlation coefficients 0.42 and -0.46, see Table 2 in the SI). The correlation coefficient we obtain between ζ_{CG} and the mobility is slightly lower than that reported by Shi et al. [23] (≈ -0.53). Yet, this difference has to be ascribed to the different water model. As a matter of fact, the calculation we perform using TIP5P provides a value in line with that of Shi et al. [23], again showing that ζ_{CG} and the NTC perform similarly (see Table 2 in the SI). Therefore, as shown in Fig. 5, using the NTC we can catch with a single order parameter both thermodynamic and dynamical anomalies.

As mentioned above and shown in our previous works [32,50], the graphs in the LDL-like state are connected graphs and near to being four-regular graphs. Accordingly, the LDL-like state is almost homogeneous in terms of connectivity. On the contrary, in the HDL-like state this regularity is partially lost: the HDL-like regime is highly heterogeneous, featuring nodes with a wide range of NTC values. Interestingly, the heterogeneity of the HDL-like regime was pointed out also using a modified version of the order parameter V_4 that goes beyond the single molecule description [76]. The LDL-like state was suggested to be composed by tetrahedral molecules that display a second-coordination shell of tetrahedral molecules (T2 molecules). The HDL-like state, instead, was suggested to be composed of molecules with distorted geometries within the first two coordination shells (D, T1 and T0 molecules).

The NTC distributions in the HDL-like regime show that there are HDL-like nodes featuring particularly high NTC values compared to the average of the HDL-like nodes at the same temperature (see Fig. 3B). In our previous work [32], we observed in the HDL-like regime, both at high pressure and at ambient conditions, the formation of extended patches of these nodes characterized by high NTC values. These patches are highly connected networks composed by nodes with an above-average connectivity and an increased number of interstitial water molecules. The analysis of water networks at ambient pressure we make here at several temperatures, confirms that the presence of these extended patches is a distinguishing feature of the HDL-like regime. We also notice the presence of small patches of nodes with an increased number of interstitial water molecules even at the lowest temperatures (i.e., below the Widom line temperature). In addition, the switch between the LDL- and HDL-like regimes by crossing the Widom line is accompanied by an abrupt change in the patches properties. To analyze these highly-connected patches, we select as nodes featuring an increased connectivity those nodes that have a number of nearest neighbors (i.e., a degree) greater than 5, as 5 is the typical number of nearest neighbors in the HDL-like states (i.e., one interstitial water molecule). Then, we define as belonging to a patch all the nodes whose degree is ≥ 6 that are linked by an edge. As it can be observed in Fig. 6, at very low temperatures there are only a few very small patches (panels A, B and D). By increasing the temperature there is a steep increase in the number of these still small patches (up to ≈20 nodes at 230 K, panels A and B) with a maximum in the number of patches at 240 K, i.e. just above the Widom line temperature. At this temperature, the most frequent patches are of the order of 15-20 molecules, but larger patches begin to appear (up to ≈50 molecules, panel E). In the HDL-like regime there is a marked increase in the patches dimension (up to ≈ 270 molecules, panel F) with a subsequent decrease in the number of patches. In the SI, Fig. 2, the plots reported in panels D to F are shown for all the simulated temperatures. It can also be observed in panel C that around the Widom line temperature the fluctuation of the patches dimension has a maximum: the coexistence of LDL- and HDL-like regions determines the coexistence of regions characterized by small and large patches, respectively. This confirms that the properties of these patches are highly related to the LDL-HDL states. Fig. 7A shows that, while these highly-connected patches are always present (the average number of patches made up of five nodes is greater than 1 for all the temperatures above 200 K, see Fig. 6A), their mean lifetime is rather small, a few ps. (Details on the mean lifetime calculation are provided in the SI, section 4). This suggests a highly dynamical scenario, in which the molecules characterized by a high connectivity are highly mobile and can easily break and form hydrogen bonds, entering and exiting the patches. Recalling that a higher connectivity is related to a higher mobility (Fig. 5A), the above defined patches appear as made of molecules with both an increased local density (high number of interstitial water molecules by construction) and an increased mobility.

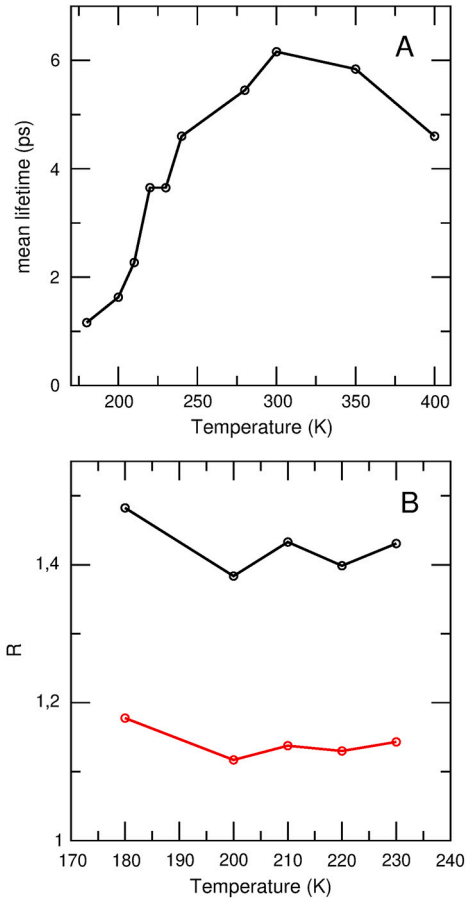

Fig. 7. A: Mean lifetime of the high connectivity patches as a function of the temperature. B: Ratio, R, between the average MSD of the nodes inside the patches and the average MSD of LDL-like (black) and HDL-like (red) nodes as a function of the temperature for temperatures below the Widom line temperature.

In Fig. 7B, we show the ratio between the mean square displacement (MSD) of the nodes belonging to the patches and that of all LDL-like nodes (black line) and HDL-like nodes (red line) for temperatures below the Widom line (more details on the calculation of the MSD are reported in the SI, section 5). It can be observed that the nodes belonging to the small patches in this temperature range are characterized by an increased mobility with respect to both the LDL- and HDL-like nodes.

A faster dynamics was already observed in molecules with an increased number of nearest neighbors [38]. Here, we show that in water at ambient pressure there are regions characterized by a higher connectivity (or communicability in the framework of graph theory) in which molecules also display an above average mobility. Recalling that the small-to-large patches transition occurs around the Widom line, we suggest that the small low-temperature patches characterized by high connectivity and mobility might be functional to the formation of extended HDL-like regions. It was recently suggested that ice nucleation occurs in low mobility regions of the LDL-like liquid [40]. In addition, Verde et al. [39] recently suggested that glassy relaxation events can be predicted by linking structure and dynamics. In analogy to these results, we suggest that the small highly connected and mobile patches might function as initial sites for the formation of extended HDL regions. This point will be further investigated in future works.

4. Conclusions

We carried out here the investigation of liquid water at ambient pressure using the node total communicability, NTC, as an order parameter. This order parameter, a centrality measure of graph theory, takes into account medium-range effects providing a measure of the connectivity of water molecules inside a network. For this investigation we use molecular dynamics simulations of TIP4P/2005 along the 1 bar isobar crossing the Widom line, going from 180 K to 400 K. Our study confirms the potentiality of the NTC in differentiating the molecules in the LDL-like state from those in the HDL-like one, and provides an estimate of the Widom line temperature in agreement with that obtained by two-state models for TIP4P/2005. However, it provides a higher LDL-like fraction at low temperatures and a lower one at high temperatures when compared to other order parameters. The origin of this difference can be ascribed to the fact that the NTC, with respect to other order parameters, is a “less local” measure, that takes into account the medium-range structural organization of the network. We also show that the NTC not only includes information about the structural aspects of the system, but is also connected to the dynamical properties of the network: molecules with higher NTC values exhibit an increased translational mobility.

We also investigated patches of connected molecules characterized by high connectivity. These structures were first identified in the HDL-like state, but here we show that they are also present in the LDL state, although less extended. These high-connectivity patches are characterized, in general, by a small lifetime and a high mobility and their size enlarges as the temperature increases, showing a correlation with the transition from the LDL- to HDL-like state. Furthermore, the small high-connectivity patches found in the LDL-like state could be the regions in which the onset of extended HDL-like regions takes place.

Declaration of competing interest

The authors declare that they have no known competing financial interests or personal relationships that could have appeared to influence the work reported in this paper.

Data availability

Data will be made available on request.

Acknowledgements

The authors wish to thank Riccardo Foffi for evaluation of the ψ order parameter on the simulation trajectories. The authors acknowledge Michele Benzi for fruitful discussions and helpful comments. ID acknowledges financial support by European Union - NextGenerationEU under the Italian Ministry of University and Research (MUR) National Innovation Ecosystem grant ECS00000041 - VITALITY - CUP E13C22001060006.

Appendix A. Supplementary material

Supplementary material related to this article can be found online at https://doi.org/10.1016/j.molliq.2023.123425.

References

[1] C. Huang, K.T. Wikfeldt, T. Tokushima, D. Nordlund, Y. Harada, U. Bergmann, M. Niebuhr, T. Weiss, Y. Horikawa, M. Leetmaa, et al., The inhomogeneous structure of water at ambient conditions, Proc. Natl. Acad. Sci. USA 106 (2009) 15214–15218.
[2] P. Gallo, J. Bachler, L.E. Bove, R. Böhmer, G. Camisasca, L.E. Coronas, H.R. Corti, I. de Almeida Ribeiro, M. de Koning, G. Franzese, et al., Advances in the study of supercooled water, Eur. Phys. J. E 44 (2021) 1–36.
[3] P. Gallo, K. Amann-Winkel, C.A. Angell, M.A. Anisimov, F. Caupin, C. Chakravarty, E. Lascaris, T. Loerting, A.Z. Panagiotopoulos, J. Russo, et al., Water: a tale of two liquids, Chem. Rev. 116 (2016) 7463–7500.
[4] R.J. Speedy, Stability-limit conjecture. An interpretation of the properties of water, J. Phys. Chem. 86 (1982) 982–991.
[5] P.H. Poole, F. Sciortino, T. Grande, H.E. Stanley, C.A. Angell, Effect of hydrogen bonds on the thermodynamic behavior of liquid water, Phys. Rev. Lett. 73 (1994) 1632.

[6] C.A. Angell, Insights into phases of liquid water from study of its unusual glass-forming properties, Science 319 (2008) 582–587.
[7] H.E. Stanley, J. Teixeira, Interpretation of the unusual behavior of h2o and d2o at low temperatures: tests of a percolation model, J. Chem. Phys. 73 (1980) 3404–3422.
[8] S. Sastry, P.G. Debenedetti, F. Sciortino, H.E. Stanley, Singularity-free interpretation of the thermodynamics of supercooled water, Phys. Rev. E 53 (1996) 6144.
[9] P.H. Poole, F. Sciortino, U. Essmann, H.E. Stanley, Phase behavior of metastable water, Nature 360 (1992) 324–328.
[10] P.H. Handle, T. Loerting, F. Sciortino, Supercooled and glassy water: metastable liquid (s), amorphous solid (s), and a no-man's land, Proc. Natl. Acad. Sci. USA 114 (2017) 13336–13344.
[11] A. Taschin, P. Bartolini, R. Eramo, R. Righini, R. Torre, Evidence of two distinct local structures of water from ambient to supercooled conditions, Nat. Commun. 4 (2013) 2401.
[12] K.H. Kim, A. Späh, H. Pathak, F. Perakis, D. Mariedahl, K. Amann-Winkel, J.A. Sellberg, J.H. Lee, S. Kim, J. Park, et al., Maxima in the thermodynamic response and correlation functions of deeply supercooled water, Science 358 (2017) 1589–1593.
[13] S. Woutersen, B. Ensing, M. Hilbers, Z. Zhao, C.A. Angell, A liquid-liquid transition in supercooled aqueous solution related to the hda-lda transition, Science 359 (2018) 1127–1131.
[14] K.H. Kim, K. Amann-Winkel, N. Giovambattista, A. Späh, F. Perakis, H. Pathak, M.L. Parada, C. Yang, D. Mariedahl, T. Eklund, et al., Experimental observation of the liquid-liquid transition in bulk supercooled water under pressure, Science 370 (2020) 978–982.
[15] F. Sciortino, I. Saika-Voivod, P.H. Poole, Study of the st2 model of water close to the liquid–liquid critical point, Phys. Chem. Chem. Phys. 13 (2011) 19759–19764.
[16] Y. Li, J. Li, F. Wang, Liquid–liquid transition in supercooled water suggested by microsecond simulations, Proc. Natl. Acad. Sci. USA 110 (2013) 12209–12212.
[17] Y. Ni, J. Skinner, Evidence for a liquid-liquid critical point in supercooled water within the e3b3 model and a possible interpretation of the kink in the homogeneous nucleation line, J. Chem. Phys. 144 (2016) 214501.
[18] P.G. Debenedetti, F. Sciortino, G.H. Zerze, Second critical point in two realistic models of water, Science 369 (2020) 289–292.
[19] V. Holten, M. Anisimov, Entropy-driven liquid–liquid separation in supercooled water, Sci. Rep. 2 (2012) 713.
[20] V. Holten, J.C. Palmer, P.H. Poole, P.G. Debenedetti, M.A. Anisimov, Two-state thermodynamics of the st2 model for supercooled water, J. Chem. Phys. 140 (2014) 104502.
[21] R.S. Singh, J.W. Biddle, P.G. Debenedetti, M.A. Anisimov, Two-state thermodynamics and the possibility of a liquid-liquid phase transition in supercooled tip4p/2005 water, J. Chem. Phys. 144 (2016) 144504, https://doi.org/10.1063/1.4944986.
[22] J.W. Biddle, R.S. Singh, E.M. Sparano, F. Ricci, M.A. Gonzalez, C. Valeriani, J.L. Abascal, P.G. Debenedetti, M.A. Anisimov, F. Caupin, Two-structure thermodynamics for the tip4p/2005 model of water covering supercooled and deeply stretched regions, J. Chem. Phys. 146 (2017) 034502.
[23] R. Shi, J. Russo, H. Tanaka, Common microscopic structural origin for water's thermodynamic and dynamic anomalies, J. Chem. Phys. 149 (2018) 224502.
[24] F. Caupin, M.A. Anisimov, Thermodynamics of supercooled and stretched water: unifying two-structure description and liquid-vapor spinodal, J. Chem. Phys. 151 (2019) 034503.
[25] F. Caupin, M.A. Anisimov, Minimal microscopic model for liquid polyamorphism and waterlike anomalies, Phys. Rev. Lett. 127 (2021) 185701.
[26] I. Daidone, R. Foffi, A. Amadei, L. Zanetti-Polzi, A statistical mechanical model of supercooled water based on minimal clusters of correlated molecules, J. Chem. Phys. 159 (2023).
[27] E. Shiratani, M. Sasai, Molecular scale precursor of the liquid–liquid phase transition of water, J. Chem. Phys. 108 (1998) 3264–3276.
[28] M.J. Cuthbertson, P.H. Poole, Mixture-like behavior near a liquid-liquid phase transition in simulations of supercooled water, Phys. Rev. Lett. 106 (2011) 115706.
[29] J. Russo, H. Tanaka, Understanding water's anomalies with locally favored structures, Nat. Commun. 5 (2014) 1–11.
[30] J.M. Montes de Oca, F. Sciortino, G.A. Appignanesi, A structural indicator for water built upon potential energy considerations, J. Chem. Phys. 152 (2020) 244503.
[31] R. Foffi, F. Sciortino, Correlated fluctuations of structural indicators close to the liquid–liquid transition in supercooled water, J. Phys. Chem. B 127 (2023) 378–386.
[32] C. Faccio, M. Benzi, L. Zanetti-Polzi, I. Daidone, Low- and high-density forms of liquid water revealed by a new medium-range order descriptor, J. Mol. Liq. 355 (2022) 118922.
[33] F. Martelli, Unravelling the contribution of local structures to the anomalies of water: the synergistic action of several factors, J. Chem. Phys. 150 (2019) 094506.
[34] R. Foffi, J. Russo, F. Sciortino, Structural and topological changes across the liquid–liquid transition in water, J. Chem. Phys. 154 (2021) 184506.
[35] J. Russo, K. Akahane, H. Tanaka, Water-like anomalies as a function of tetrahedrality, Proc. Natl. Acad. Sci. USA 115 (2018) E3333–E3341.
[36] R. Shi, J. Russo, H. Tanaka, Origin of the emergent fragile-to-strong transition in supercooled water, Proc. Natl. Acad. Sci. USA 115 (2018) 9444–9449.
[37] J.M. Montes de Oca, S.R. Accordino, G.A. Appignanesi, P.H. Handle, F. Sciortino, Size dependence of dynamic fluctuations in liquid and supercooled water, J. Chem. Phys. 150 (2019) 144505.
[38] F. Sciortino, A. Geiger, H.E. Stanley, Effect of defects on molecular mobility in liquid water, Nature 354 (1991) 218–221.
[39] A.R. Verde, L.M. Alarcón, G.A. Appignanesi, Correlations between defect propensity and dynamical heterogeneities in supercooled water, J. Chem. Phys. 158 (2023).
[40] M. Fitzner, G.C. Sosso, S.J. Cox, A. Michaelides, Ice is born in low-mobility regions of supercooled liquid water, Proc. Natl. Acad. Sci. USA 116 (2019) 2009–2014.
[41] T. Speck, A. Malins, C.P. Royall, First-order phase transition in a model glass former: coupling of local structure and dynamics, Phys. Rev. Lett. 109 (2012) 195703.
[42] M. Leocmach, H. Tanaka, Roles of icosahedral and crystal-like order in the hard spheres glass transition, Nat. Commun. 3 (2012) 974.
[43] A. Malins, J. Eggers, C.P. Royall, S.R. Williams, H. Tanaka, Identification of long-lived clusters and their link to slow dynamics in a model glass former, J. Chem. Phys. 138 (2013) 12A535.
[44] H. Tong, H. Tanaka, Structural order as a genuine control parameter of dynamics in simple glass formers, Nat. Commun. 10 (2019) 5596.
[45] S. Marín-Aguilar, H.H. Wensink, G. Foffi, F. Smallenburg, Slowing down supercooled liquids by manipulating their local structure, Soft Matter 15 (2019) 9886–9893.
[46] S. Marín-Aguilar, H.H. Wensink, G. Foffi, F. Smallenburg, Tetrahedrality dictates dynamics in hard sphere mixtures, Phys. Rev. Lett. 124 (2020) 208005.
[47] E. Boattini, S. Marín-Aguilar, S. Mitra, G. Foffi, F. Smallenburg, L. Filion, Autonomously revealing hidden local structures in supercooled liquids, Nat. Commun. 11 (2020) 5479.
[48] E. Boattini, F. Smallenburg, L. Filion, Averaging local structure to predict the dynamic propensity in supercooled liquids, Phys. Rev. Lett. 127 (2021) 088007.
[49] J. Abascal, C. Vega, A general purpose model for the condensed phases of water: Tip4p/2005, J. Chem. Phys. 123 (2005) 234505.
[50] M. Benzi, I. Daidone, C. Faccio, L. Zanetti-Polzi, Structural analysis of water networks, J. Complex Netw. 11 (2023) cnad001.
[51] E. Estrada, The Structure of Complex Networks: Theory and Applications, Oxford University Press, 2012.
[52] M. Benzi, C. Klymko, Total communicability as a centrality measure, J. Complex Netw. 1 (2013) 124–149.
[53] E. Estrada, N. Hatano, M. Benzi, The physics of communicability in complex networks, Phys. Rep. 514 (2012) 89–119.
[54] M. Benzi, C. Klymko, On the limiting behavior of parameter-dependent network centrality measures, SIAM J. Matrix Anal. Appl. 36 (2015) 686–706.
[55] P. Bonacich, Power and centrality: a family of measures, Am. J. Sociol. 92 (1987) 1170–1182.
[56] D. Schlesinger, K.T. Wikfeldt, L.B. Skinner, C.J. Benmore, A. Nilsson, L.G. Pettersson, The temperature dependence of intermediate range oxygen-oxygen correlations in liquid water, J. Chem. Phys. 145 (2016).
[57] K.T. Wikfeldt, C. Huang, A. Nilsson, L.G. Pettersson, Enhanced small-angle scattering connected to the Widom line in simulations of supercooled water, J. Chem. Phys. 134 (2011).
[58] P.G. Debenedetti, Supercooled and glassy water, J. Condens. Matter Phys. 15 (2003) R1669.
[59] J. Abascal, C. Vega, Widom line and the liquid–liquid critical point for the tip4p/2005 water model, J. Chem. Phys. 133 (2010) 234502.
[60] T. Sumi, H. Sekino, Effects of hydrophobic hydration on polymer chains immersed in supercooled water, RSC Adv. 3 (2013) 12743–12750.
[61] M.J. Abraham, T. Murtola, R. Schulz, S. Páll, J.C. Smith, B. Hess, E. Lindahl, Gromacs: high performance molecular simulations through multi-level parallelism from laptops to supercomputers, SoftwareX 1 (2015) 19–25.
[62] G. Bussi, D. Donadio, M. Parrinello, Canonical sampling through velocity rescaling, J. Chem. Phys. 126 (2007) 014101.
[63] M. Parrinello, A. Rahman, Crystal structure and pair potentials: a molecular-dynamics study, Phys. Rev. Lett. 45 (1980) 1196.
[64] T. Darden, D. York, L. Pedersen, Particle mesh Ewald: an nlog (n) method for Ewald sums in large systems, J. Chem. Phys. 98 (1993) 10089–10092.
[65] B. Hess, H. Bekker, H.J. Berendsen, J.G. Fraaije, Lincs: a linear constraint solver for molecular simulations, J. Comput. Chem. 18 (1997) 1463–1472.
[66] A. Hagberg, D.S. Chult, P. Swart, Exploring network structure, dynamics, and function using networkx, in: G. Varoquaux, T. Vaught, J. Millman (Eds.), Proceedings of the 7th Python in Science Conference, Pasadena, CA USA, 2008, pp. 11–15.
[67] N. Michaud-Agrawal, E.J. Denning, T.B. Woolf, O. Beckstein, Mdanalysis: a toolkit for the analysis of molecular dynamics simulations, J. Comput. Chem. 32 (2011) 2319–2327.
[68] R.J. Gowers, M. Linke, J. Barnoud, T.J. Reddy, M.N. Melo, S.L. Seyler, J. Domanski, D.L. Dotson, S. Buchoux, I.M. Kenney, et al., Mdanalysis: a python package for the rapid analysis of molecular dynamics simulations, in: Proceedings of the 15th Python in Science Conference, vol. 98, SciPy, Austin, TX, 2016, p. 105.
[69] A. Bucci, Networksns, https://doi.org/10.5281/zenodo.8073704, 2023.
[70] C.R. Harris, S.J. Millman, K.J. Van Der Walt, R. Gommers, P. Virtanen, D. Cournapeau, E. Wieser, J. Taylor, S. Berg, N.J. Smith, R. Kern, M. Picus, S. Hoyer, M.H. van Kerkwijk, M. Brett, A. Haldane, J.F. del Río, M. Wiebe, P. Peterson, P. Gérard-Marchant, K. Sheppard, R. T., W. Weckesser, H. Abbasi, C. Gohlke, T.E. Oliphant, Array programming with NumPy, Nature 585 (2020) 357–362, https://doi.org/10.1038/s41586-020-2649-2.
[71] P. Virtanen, R. Gommers, T.E. Oliphant, M. Haberland, T. Reddy, D. Cournapeau, E. Burovski, W. Peterson, P.Weckesser, J. Bright, S.J. van der Walt, M. Brett, J. Wilson, K.J. Millman, N. Mayorov, A.R.J. Nelson, E. Jones, R. Kern, E. Larson, C.J.

Carey, İ. Polat, Y. Feng, E.W. Moore, J. VanderPlas, D. Laxalde, J. Perktold, R. Cimrman, I. Henriksen, E.A. Quintero, C.R. Harris, A.M. Archibald, A.H. Ribeiro, F. Pedregosa, P. van Mulbregt, SciPy 1.0 contributors, SciPy 1.0: fundamental algorithms for scientific computing in python, Nat. Methods 17 (2020) 261–272, https://doi.org/10.1038/s41592-019-0686-2.

[72] J.D. Hunter, Matplotlib: a 2d graphics environment, Comput. Sci. Eng. 9 (2007) 90–95, https://doi.org/10.1109/MCSE.2007.55.

[73] C. Vega, J.L.F. Abascal, I. Nezbeda, Vapor-liquid equilibria from the triple point up to the critical point for the new generation of TIP4P-like models: TIP4P/Ew, TIP4P/2005, and TIP4P/ice, J. Chem. Phys. 125 (2006) 034503.

[74] P. Kumar, K.T. Wikfeldt, D. Schlesinger, L.G. Pettersson, H.E. Stanley, The boson peak in supercooled water, Sci. Rep. 3 (2013) 1980.

[75] L. Zanetti-Polzi, I. Daidone, A. Amadei, A general statistical mechanical model for fluid system thermodynamics: application to sub- and super-critical water, J. Chem. Phys. 156 (2022) 044506.

[76] N.A. Loubet, A.R. Verde, J.A. Lockhart, G.A. Appignanesi, Turning an energy-based defect detector into a multi-molecule structural indicator for water, J. Chem. Phys. 159 (2023).